An electron paramagnetic resonance study of vanadium centres in $RbZnF_3$ single crystals

2008 J. Phys.: Condens. Matter 20 055221

(http://iopscience.iop.org/0953-8984/20/5/055221)

J. Phys.: Condens. Matter **20** (2008) 055221 (7pp) doi:10.1088/0953-8984/20/5/055221

An electron paramagnetic resonance study of vanadium centres in $RbZnF_3$ single crystals

H Takeuchi[1], **H Ebisu**[2] **and M Arakawa**[3,4]

[1] Department of Advanced Science and Technology, Toyota Technological Institute, Nagoya 468-8511, Japan
[2] Department of Electrical and Computer Engineering, Nagoya Institute of Technology, Nagoya 466-8555, Japan
[3] Department of Materials Science and Engineering, Nagoya Institute of Technology, Nagoya 466-8555, Japan

Received 4 October 2007, in final form 20 December 2007
Published 18 January 2008
Online at stacks.iop.org/JPhysCM/20/055221

Abstract

Electron paramagnetic resonance (EPR) measurements have been made at room temperatures for sample crystals of $RbZnF_3$ doped only with vanadium and codoped with vanadium and lithium. For the V-only-doped crystal, two kinds of EPR spectra having eight-line hyperfine structure ($I = \frac{7}{2}$) were observed. One spectrum with cubic symmetry is ascribed to a V^{2+} ion ($S = \frac{3}{2}$) substituting for a host Zn^{2+} ion. The other spectrum with tetragonal symmetry is ascribed to a V^{4+}–O^{2-} pair ($S = \frac{1}{2}$) substituting for the host Zn^{2+}–F^- pair in the cubic perovskite phase of the matrix crystal. In the V, Li-codoped crystal, two kinds of new EPR spectra having monoclinic symmetry with $S = \frac{1}{2}$ and $I = \frac{7}{2}$ were observed, and no V^{2+} centres were observed. The new spectra are ascribed to $VLiOF_8$ complexes formed at Zn_2F_9 units in the hexagonal $BaTiO_3$ type phase of the matrix crystal. In these centres, excess divalent positive charges on the V^{4+} ions are compensated justly by forming V^{4+}–Li^+–O^{2-} structures. It is confirmed from the results that the hexagonal $BaTiO_3$ type high temperature phase of $RbZnF_3$ can be stabilized even in the temperature region of the cubic perovskite type phase of pure $RbZnF_3$ crystal by the preferential formation of V^{4+}–Li^+ pairs at the hexagonal Zn_2F_9 units.

1. Introduction

It is known that the crystal structure of ABF_3 compound is related to the tolerance factor $t = (r_A + r_F)/\sqrt{2}\,(r_B + r_F)$ where r_A, r_B and r_F are respectively the ionic radii of the A^+, B^{2+} and F^- ions. The cubic perovskite type structure is stable for compounds with $t = 0.88$–1.00, and the hexagonal $BaTiO_3$ type structure is stable for compounds with $t = 1.00$–1.06 [1, 2]. The fluoride $RbZnF_3$ is the compound on the boundary of these two types of structure as its tolerance factor is 1.00. In fact, it was reported that $RbZnF_3$ crystallizes at about 730 °C from a melt into the hexagonal $BaTiO_3$ type structure and undergoes structural phase transition at about 640 °C into the cubic perovskite structure on cooling temperature [3].

[4] Present Address: Nakagawa-ku, Nagoya 454-0817, Japan.

Figure 1 shows the hexagonal $BaTiO_3$ type structure of $RbZnF_3$ crystal. This structure has two kinds of Zn^{2+} sites. One is the Zn^{2+} site in the ZnF_6 unit where the Zn^{2+} ion situates at the centre of a single fluorine octahedron which is connected to other octahedra at the six vertices of the octahedron. We denote this type of Zn^{2+} site as the Zn_I site hereafter. The other is the Zn^{2+} site in the Zn_2F_9 unit where two fluorine octahedra are connected by sharing one face of fluorine triangle. We denote this type of Zn^{2+} site as the Zn_{II} site hereafter. Two neighbouring Zn_{II} sites line along the crystalline c axis. Figure 2 shows the projections of the arrangement of these two types of Zn^{2+} site onto the planes normal to the a' or c axes.

In the previous works of EPR results on the Cr^{3+} and Gd^{3+} centres in $RbZnF_3$ single crystals [4, 5], it is reported that $RbZnF_3$ crystals have the cubic perovskite type structure at room temperatures the same as the pure crystal when only Cr^{3+}

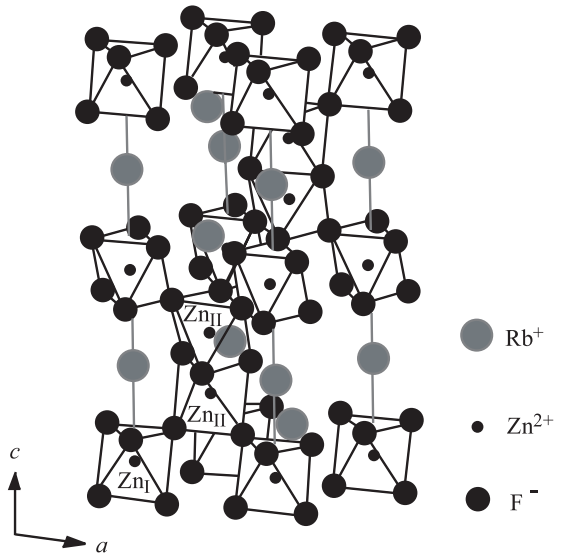

Figure 1. Structure of $RbZnF_3$ crystal in the hexagonal $BaTiO_3$ type phase. Two types of Zn^{2+} site are denoted by Zn_I and Zn_{II}.

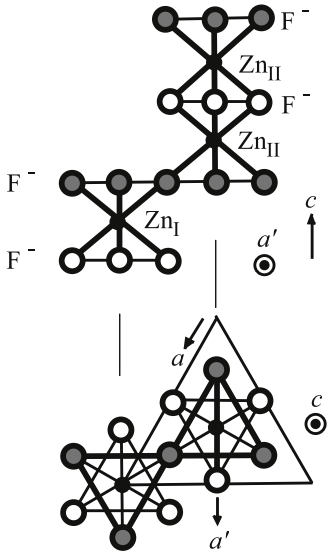

Figure 2. Definitions of the crystalline a, a' and c axis directions in the hexagonal $RbZnF_3$ crystal.

or Gd^{3+} is doped. There, it is found that some $RbZnF_3$ crystals have anomalously the hexagonal $BaTiO_3$ type structure even at room temperatures when Cr^{3+} or Gd^{3+} ions are codoped with Li^+ ions.

In the present work, we carried out EPR measurements on the $RbZnF_3$ single crystals doped with vanadium and codoped with vanadium and lithium to confirm the important role of Li^+ ion in the anomalous stability of the high temperature phase of $RbZnF_3$ crystal at room temperatures. Several EPR spectra of vanadium ions were observed at room temperatures. In section 3, we will analyse angular variations of the spectra by matrix diagonalization on a computer to obtain accurate spin Hamiltonian parameters for these spectra. In section 4, we will discuss the structure of each vanadium centre. It will be shown by charge-compensation considerations and the analyses of hyperfine parameters that the hexagonal $BaTiO_3$ type crystal structure becomes stable even at room temperatures when V^{4+} ions associate with Li^+ ions in the form of justly charge-compensated V^{4+}–Li^+–O^{2-} structures.

2. Experimental procedures

Single crystals of $RbZnF_3$ doped with vanadium were grown by the Bridgman technique. Starting mixtures of RbF and ZnF_2 powders and about 0.1 mol% of $VOSO_4{\cdot}2H_2O$ were sealed in glassy carbon crucibles. The crucible was heated to 800 °C to yield liquid mixture. Then the temperature of the crucible was lowered slowly to 300 °C with a cooling rate of about 50 °C h^{-1}. Single crystals of $RbZnF_3$ having natural planes of cubic structure were grown in the batch doped only with vanadium. In some starting mixtures about 0.5 mol% of LiF powder was added. In the batch codoped with vanadium and lithium, single crystals having natural planes of hexagonal structure were grown. Sample crystals having natural planes of cubic and hexagonal structures were obtained from respective batches for the EPR experiments.

The EPR measurements were carried out at room temperature using a JES-FE1XG X-band spectrometer (JEOL) with 100 kHz field modulation at the Advanced Instrument and Analysis Division in Nagoya Institute of Technology. To observe angular variation of spectra the sample crystals were rotated in the cylindrical microwave cavity with TE_{011} mode. An NMR probe (Echo Electronics) was used for accurate measurements of the magnetic field. X-ray diffraction analyses for powdered samples were performed with Cu Kα radiation using the spectrometer at the Advanced Instrument and Analysis Division in Nagoya Institute of Technology.

3. Results

Figure 3 is recorder traces of EPR signals observed at room temperature from $RbZnF_3$ single crystal doped only with vanadium. The spectra are composed of the signals with eight-line hyperfine structure indicated by small vertical bars and the signals marked with A. Figures 4 and 5 show angular variation of the spectrum for above crystal with $\boldsymbol{H}$ in the (001) and the $(1\bar{1}0)$ planes, respectively. The resonant fields of the signals with the eight-line hyperfine structure indicated by the small vertical bars have no angular dependences on the external field direction. The hyperfine splitting is very close to those for the V^{2+} centres formed in the perovskite matrices $KMgF_3$ and $KZnF_3$ [6, 7], where the V^{2+} ions are coordinated by six fluorine ligands. The comparison of the hyperfine parameters will be given in table 2 in section 4. Thus, it is reasonable from the magnitude of the hyperfine structure splitting with the nuclear spin $I = \frac{7}{2}$ that the signals are due to a $V^{2+}(3d^3)$ ion with the electronic spin $S = \frac{3}{2}$. As the resonant field positions for the hyperfine structure have no angular dependences in the (001) and $(1\bar{1}0)$ rotation planes, the V^{2+} ion is confirmed to be at a site with cubic symmetry. The spectrum can be ascribed to a V^{2+} ion substituting for a Zn^{2+} ion of $RbZnF_3$ crystal in the cubic perovskite type phase. The cubic perovskite structure

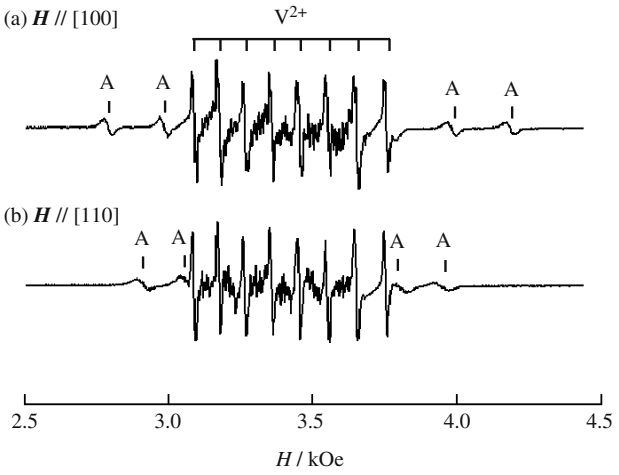

Figure 3. X-band EPR spectra observed at 300 K for $RbZnF_3$ doped only with vanadium with (a) $\boldsymbol{H} \parallel [100]$ axis and (b) $\boldsymbol{H} \parallel [110]$ axis. Signals marked with a set of eight bars are those from a V^{2+} ion. The superhyperfine structures seen in the field range of 3.1–3.6 kOe are due to Mn^{2+} ions substituting at the Zn^{2+} sites having cubic symmetry.

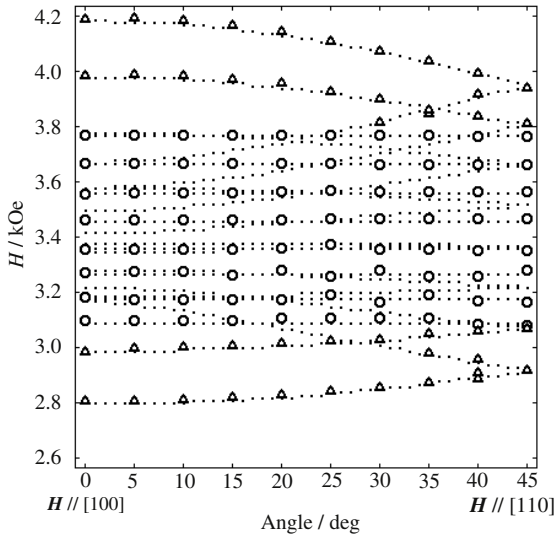

Figure 4. Angular variations of the signals in figure 3 with $\boldsymbol{H}$ in the (001) plane. Open circles and open triangles denote, respectively, the experimental resonant fields for the V^{2+} centre and centre A. Dotted lines show the theoretical resonant fields calculated with the parameters in table 1.

of the vanadium-only-doped crystal was also confirmed by x-ray diffraction analysis for a powdered sample. Thus, the V^{2+} is identified to be forming VF_6 complex in the cubic $RbZnF_3$ crystal.

The angular variation of the signals A in figures 4 and 5 showed no fine structure splitting except for the anisotropic hyperfine structure due to the interaction of a 3d electron with the self-nucleus, so that the spectrum composed of the signals marked with A in figure 3 is considered to be due to a vanadium ion with $S = \frac{1}{2}$ and $I = \frac{7}{2}$. The spectra of the signals A in the [100], [010] and [001] field directions were equivalent, and as

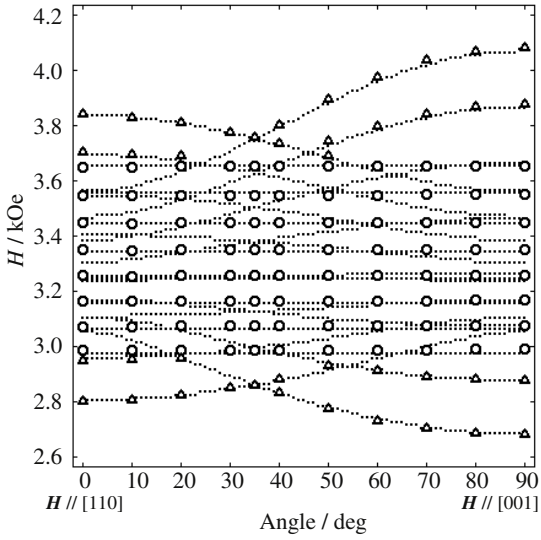

Figure 5. Angular variations of the signals in figure 3 with $\boldsymbol{H}$ in the (110) plane. The notation is the same as that for figure 4. Microwave frequency is different from that in figure 4.

shown in figure 5 their signal branches crossed to each other in the [111] direction. In the [110] field direction in figure 4, the signal branch having a peak in the [100] direction coincides with the branch which has a trough in the [100] direction and has a peak in the [010] direction. These results indicate that the spectrum has tetragonal symmetry about one of the ⟨100⟩ axes (called centre A hereafter). From the value of electronic spin $S = \frac{1}{2}$, the vanadium is considered to be in a $V^{4+}(3d^1)$ state. The tetragonal symmetry of centre A suggests the existence of some charge compensator associated to the vanadium.

The vanadium superhyperfine structures on the signals marked with A in figures 3(a) and (b) are faint. The sample crystal includes a small amount of Mn^{2+} ions unexpectedly. The superhyperfine structures seen in the field range of about 3.1–3.6 kOe in both figures are ascribed to the Mn^{2+} ions substituting for Zn^{2+} ions since the superhyperfine splitting of about 18 Oe and the total field range of the spectrum are the same as those for the Mn^{2+} spectrum observed in the cubic $RbZnF_3$ crystal with more concentrated Mn^{2+} ions substituting at the Zn^{2+} sites having cubic symmetry.

Figure 6 shows recorder traces of EPR signals observed at room temperature for $RbZnF_3$ crystal codoped with vanadium and lithium. Some new vanadium signals marked with B and C are seen in the spectra. Figures 7 and 8 show angular variations of the spectrum of the vanadium signals. In figure 8, extremes of the EPR branches appear at intervals of 60°. This angular variation of the spectrum shows that the host crystal is in the hexagonal $BaTiO_3$ type phase. The hexagonal structure of the matrix crystal codoped with vanadium and lithium was also confirmed by x-ray diffraction analysis for a powdered sample.

The spectra for the signals B and C showed no fine structure splittings in spite of their low symmetry. It is found from this behaviour of the angular variations of the spectra that both spectra for the signals B and C have electronic spin $S = \frac{1}{2}$ and nuclear spin $I = \frac{7}{2}$ (called centres B and C hereafter).

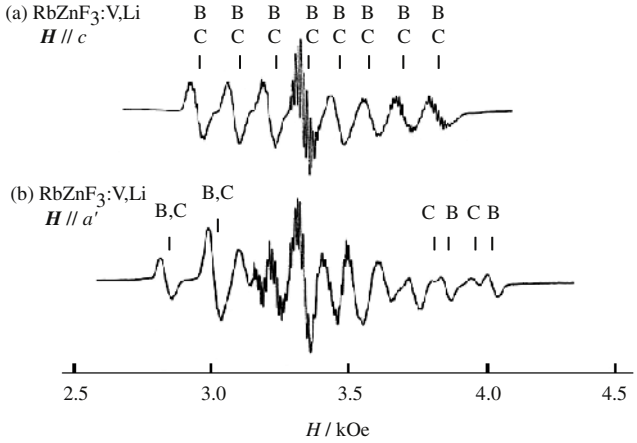

Figure 6. EPR spectra observed at 300 K from $RbZnF_3$ codoped with vanadium and lithium (a) when $\boldsymbol{H} \parallel c$, and (b) when $\boldsymbol{H} \parallel a'$. The superhyperfine structures are due to a Mn^{2+} axial centre.

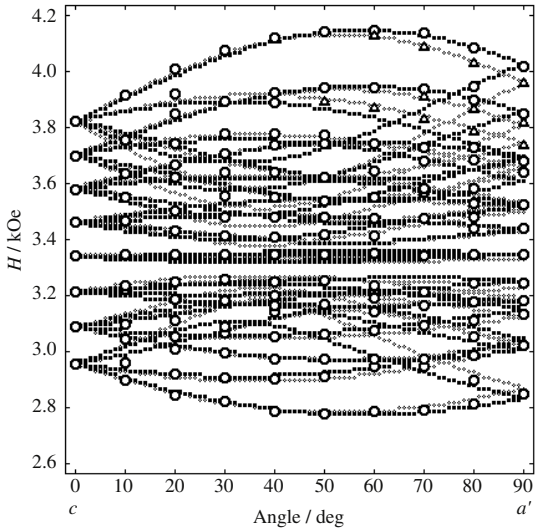

Figure 7. Angular variations of the signals of centres B and C with $\boldsymbol{H}$ rotated from the c axis to the a' axis. Observed signals are denoted by open circles and triangles, respectively, for centres B and C. The dots denote theoretical resonant fields.

The vanadium ions of these centres are considered to be in the $V^{4+}(3d^1)$ states. When $\boldsymbol{H} \parallel c$, the signals of centre C overlap on the signals of centre B. In the external field directions near a or a' axes, several signals of centre C are observed separately from the signals of centre B in the high field region. The signals of centre B are stronger than the corresponding signals of centre C as seen from figure 6(b). It should be noted that any V^{2+} centres were not observed from V, Li-codoped crystals contrary to the case of V-only-doped crystals.

The sample crystal includes Mn^{2+} ions a little as the case of the cubic $RbZnF_3$ sample. The axially symmetric Mn^{2+} spectrum which has been observed in the more concentrated hexagonal $RbZnF_3$ crystal extends over the range of 2.8–4.1 kOe for $\boldsymbol{H} \parallel c$. Its superhyperfine structures with the splitting of about 18 Oe are seen in the spectra of figures 6(a) and (b). Similar superhyperfine structure is reported for the Mn^{2+} centre in the hexagonal $RbMgF_3$ crystal [8].

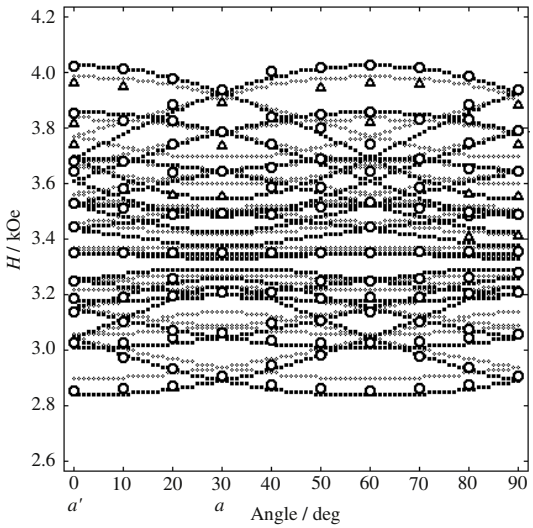

Figure 8. Angular variations of the signals of centres B and C with $\boldsymbol{H}$ rotated from the a' axis toward the a axis in the c plane. The notation is the same as that for figure 7.

Here, we analyse the observed spectra of the V^{2+} centre and the V^{4+} centres A, B and C using the spin Hamiltonians composed of Zeeman Hamiltonian $\mathcal{H}_Z$ and hyperfine structure Hamiltonian $\mathcal{H}_{HFS}$ adapted for each symmetry. The EPR spectrum of the V^{2+} centre in the cubic perovskite type $RbZnF_3$ crystal can be described by the following spin Hamiltonian:

$$\mathcal{H} = g\beta \boldsymbol{S} \cdot \boldsymbol{H} + A\boldsymbol{S} \cdot \boldsymbol{I}, \tag{1}$$

where $S = \frac{3}{2}$, $I = \frac{7}{2}$, $g = g_x = g_y = g_z$, $A = A_x = A_y = A_z$ and β is Bohr magneton. The x, y and z axes are chosen to be parallel to the cubic axes. The EPR spectrum of centre A can be described by the following spin Hamiltonian:

$$\mathcal{H} = g_\parallel \beta S_z H_z + g_\perp \beta (S_x H_x + S_y H_y) + A_\parallel S_z I_z + A_\perp (S_x I_x + S_y I_y), \tag{2}$$

where $S = \frac{1}{2}$, $I = \frac{7}{2}$, $g_\parallel = g_z$, $g_\perp = g_x = g_y$, $A_\parallel = A_z$ and $A_\perp = A_x = A_y$. The z axis is chosen to be parallel to the tetragonal axis.

The spectra of centres B and C have a monoclinic symmetry plane (ca' plane). We choose the z- and x-axis directions in this symmetry plane. When the z-axis direction do not coincide with the main principal axis direction of Zeeman or hyperfine matrices in the spin Hamiltonian, these matrices include off-diagonal zx and xz components. If we select the z-axis direction to coincide with the main principal axis direction in the symmetry plane, the matrix with monoclinic symmetry can be diagonalized into one with orthorhombic symmetry. The principal axis direction for the Zeeman matrix is not necessarily the same as that for the hyperfine matrix. As will be seen in table 2 in section 4, the anisotropy in the Zeeman term is rather small compared with the anisotropy in the hyperfine term, so we choose the z-axis direction so that the hyperfine term is expressed in a diagonal form and adopt the approximation where the off-diagonal elements of Zeeman

Table 1. Spin Hamiltonian parameters obtained at 300 K for the observed vanadium centres in $RbZnF_3$. Units are in 10^{-4} cm^{-1} for A_x, A_y and A_z.

Centre	g_x	g_y	g_z	A_x	A_y	A_z	θ (deg)
V-doped							
V^{2+} centre	1.9658(3)	1.9658(3)	1.9658(3)	−87.0(1)	−87.0(1)	−87.0(1)	—
Centre A	1.9682(4)	1.9682(4)	1.9327(2)	−66.3(4)	−66.3(4)	−178.92(6)	—
V, Li-doped							
Centre B	1.9696(6)	1.9708(12)	1.9339(8)	−74.1(6)	−41(3)	−176.9(3)	57.8(5)
Centre C	1.971(2)	1.971(2)	1.936(1)	−52(3)	−73(2)	−174(2)	52.7(5)

Table 2. Calculated values of g_s, g_p, g_r, A_s, A_p and A_r for the vanadium centres observed in $RbZnF_3$ crystals. The values for the V^{2+} centres formed in $KMgF_3$ and $KZnF_3$ and those for the $[VOF_5]^{3-}$ centre in $KZnF_3$ are listed for comparison. Units are in 10^{-4} cm^{-1} for A_s, A_p and A_r.

Centre	g_s	g_p	g_r	A_s	A_p	A_r
V-doped $RbZnF_3$						
V^{2+} centre	1.9658	—	—	−87.0	—	—
Centre A	1.9564	−0.0118	—	−103.8	−37.5	—
V, Li-codoped $RbZnF_3$						
Centre B	1.9581	−0.0121	−0.0006	−97.3	−39.8	−16.6
Centre C	1.959	−0.012	0.000	−100	−37	11
$KMgF_3$:V^{2+} [6]	1.9720	—	—	−86.3	—	—
$KZnF_3$:V^{2+} [7]	1.972	—	—	−86.2	—	—
$KZnF_3$:$[VOF_5]^{3-}$ [9]	1.9737	−0.0203	—	103.0	37.8	—

matrix are neglected. Thus, the EPR spectra of centres B and C were described by the following spin Hamiltonian:

$$\mathcal{H} = g_x\beta S_x H_x + g_y\beta S_y H_y + g_z\beta S_z H_z + A_x S_x I_x + A_y S_y I_y + A_z S_z I_z, \quad (3)$$

where $S = \frac{1}{2}$ and $I = \frac{7}{2}$. The z axis is declined by an angle θ from the crystalline c axis toward the a' axis of the hexagonal $RbZnF_3$ crystal. The x axis is in the ca' plane. For the resonant fields used for parameter fitting, accurate measurements were made using the NMR probe in the best-set field directions. The spin Hamiltonian parameters were fitted to the spectra by matrix diagonalization on a computer. Obtained parameters are tabulated in table 1. In figures 7 and 8, the lines by dots denote the resonant fields calculated theoretically for centres B and C using the determined spin Hamiltonian parameters in table 1.

4. Discussions

The Zeeman Hamiltonian $\mathcal{H}_Z$ can be represented by the sum of isotropic, axial and rhombic terms as follows:

$$\mathcal{H}_Z = g_s\beta \boldsymbol{S}\cdot\boldsymbol{H} + g_p\beta(3S_z H_z - \boldsymbol{S}\cdot\boldsymbol{H}) + g_r\beta(S_x H_x - S_y H_y). \quad (4)$$

The parameters g_s, g_p and g_r are calculated using the following equations:

$$g_s = \tfrac{1}{3}(g_x + g_y + g_z), \quad (5)$$

$$g_p = \frac{1}{3}\left(g_z - \frac{g_x + g_y}{2}\right), \quad (6)$$

$$g_r = \tfrac{1}{2}(g_x - g_y). \quad (7)$$

Similarly, the hyperfine structure Hamiltonian $\mathcal{H}_{HFS}$ can be represented by the sum of isotropic, axial and rhombic terms as follows:

$$\mathcal{H}_{HFS} = A_s\boldsymbol{S}\cdot\boldsymbol{I} + A_p(3S_z I_z - \boldsymbol{S}\cdot\boldsymbol{I}) + A_r(S_x I_x - S_y I_y). \quad (8)$$

The parameters A_s, A_p and A_r are calculated using the following equations:

$$A_s = \tfrac{1}{3}(A_x + A_y + A_z), \quad (9)$$

$$A_p = \frac{1}{3}\left(A_z - \frac{A_x + A_y}{2}\right), \quad (10)$$

$$A_r = \tfrac{1}{2}(A_x - A_y). \quad (11)$$

Values of g_s, g_p, g_r, A_s, A_p and A_r calculated from the values of the spin Hamiltonian parameters in table 1 are tabulated in table 2.

As seen from the table, the isotropic parts of the g tensor for centres A, B and C are about 0.01 smaller than the typical value $g_s \simeq 1.97$ for the V^{2+} centres formed in the perovskite fluorides $KMgF_3$ and $KZnF_3$ [6, 7]. The axial parts of the g tensor for centres A, B and C have considerably large magnitudes and are almost the same for three centres although the symmetry of centre A is different from those of centres B and C.

Absolute signs of the hyperfine parameters in table 1 can be determined by considering the fact that dominant isotropic part of the central hyperfine interaction arises from Fermi-contact interaction with the self-nucleus through the core-polarization mechanism [10]. The value of A_s is expected to be different among the different valence vanadium ions. In fact, as seen from table 2, the magnitudes of A_s for centres A, B and C are about 10×10^{-4} cm^{-1} larger than that for the

V^{2+} centre although the signs of A_s are commonly negative among the four centres. On the other hand, the axial parts of the hyperfine structure Hamiltonians are almost the same for centres A, B and C and have considerably large ratio to A_s, that is $A_p/A_s \simeq 0.4$. The large axiality of the hyperfine interaction comes from the $3d^1$ electronic state of a V^{4+} ion in contrast with the $3d^3$ electronic state of a V^{2+} ion. This $V^{4+}(3d^1)$ state may be stabilized by the existence of common charge compensator creating strong axial field at the vanadium ion sites to compensate the excess positive charge on the V^{4+} ions substituting for the host Zn^{2+} ions.

Centre A with the spins $S = \frac{1}{2}$ and $I = \frac{7}{2}$ has tetragonal symmetry about one of the ⟨100⟩ axes of the cubic perovskite type crystal. The electronic spin $\frac{1}{2}$ corresponds to a V^{4+} ion with $3d^1$ configuration although the spectrum of this centre was observed at room temperatures. It is reported that EPR spectra from V^{4+} ions in strong axial field can be observed even at room temperature for their long spin–lattice relaxation time [11]. As the crystals were doped with $VOSO_4{\cdot}2H_2O$ powder, centre A may be ascribed to a V^{4+}–O^{2-} pair substituting for a Zn^{2+}–F^- pair of the cubic perovskite type $RbZnF_3$ crystal. Buzaré *et al* [9] reported EPR results for an axial vanadium centre formed in $KZnF_3$ crystal as the $[VOF_5]^{3-}$ centre, where V^{4+}–O^{2-} ion pair may be substituting for the host Zn^{2+}–F^- ion pair. The magnitudes of A_s and A_p for $[VOF_5]^{3-}$ centre in $KZnF_3$ listed in table 2 are close to the respective values for centre A in $RbZnF_3$. Thus, in both the matrices of cubic perovskite crystals $RbZnF_3$ and $KZnF_3$, the vanadium ions are considered to be in the $V^{4+}(3d^1)$ state. It should be pointed out that the signs of A_s are negative due to the main core-polarization mechanism although some papers up to now reported erroneous positive values for the hyperfine parameters [9, 12–14].

In the previous works for $RbZnF_3$ codoped with Li^+ ions together with Cr^{3+} or Gd^{3+} ions [4, 5], it is found that the hexagonal $BaTiO_3$ type structure is anomalously stabilized by the formation of M^{3+}–Li^+ pairs (M = Cr, Gd) substituting for Zn^{2+}–Zn^{2+} pairs in the Zn_2F_9 units. From sample crystals of $RbZnF_3$ codoped with vanadium and lithium in the present work, no signals of V^{2+} centres were observed. Instead, the strong signals from the V^{4+} centres B and C with monoclinic symmetry in the hexagonal $BaTiO_3$ type structure were observed. This fact supports that preferential formation of V^{4+}–Li^+ pairs substituting for Zn^{2+}–Zn^{2+} pairs in the Zn_2F_9 units take place in the V, Li-codoped crystal and stabilize the hexagonal structure even at room temperatures. The V^{4+}–Li^+ pairs may maintain tightly the face-sharing structures of two surrounding fluorine octahedra and act against the reformation of the matrix crystal from hexagonal to cubic perovskite structure on lowering temperature from high temperature phase.

As a V^{4+}–Li^+ pair substituting for a Zn^{2+}–Zn^{2+} pair has excess positive charge in contrast with justly charge-compensated M^{3+}–Li^+ pairs (M = Cr, Gd) formed at a Zn_2F_9 unit, V^{4+} ions in centres B and C are considered to be associating with some additional charge compensators which make the centres to have monoclinic symmetry. Although the host Zn_{II} site has trigonal symmetry about the c axis, centres B and C have axialities along the directions declined by the angles θ (≃53°) from the c axis. This indicates the existence of charge compensator with strong axiality along the declined direction. We may consider that V^{4+}–Li^+ pairs at the Zn_{II}–Zn_{II} sites are associating with O^{2-} ions substituting for one of the nearest F^- ions. Thus, centres B and C may be ascribed to $VLiOF_8$ complexes in the Zn_2F_9 units in hexagonal $RbZnF_3$ crystal.

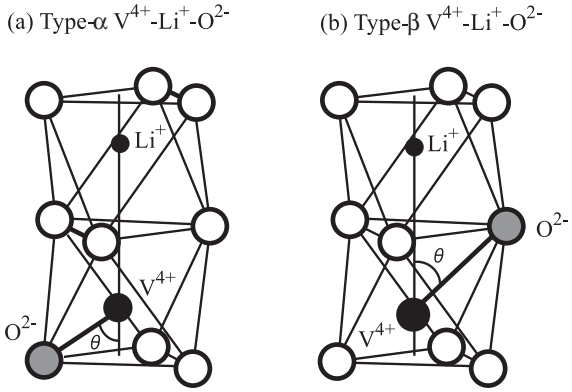

Figure 9. Schematic models of the $VLiOF_8$ complexes of (a) type α and (b) type β to be formed in the hexagonal $RbZnF_3$ crystal codoped with vanadium and lithium.

Since the $VLiOF_8$ complexes have the same valence as Zn_2F_9, the divalent excess positive charge on the vanadium ion is compensated justly by Li^+ and O^{2-} ions so that centres B and C become stable. Figure 9 shows two types of $VLiOF_8$ complex to be formed in the hexagonal $RbZnF_3$ crystal. The vanadium and lithium ions substitute for the Zn_{II}–Zn_{II} pair. Two types of $VLiOF_8$ complex are distinguished by the position of the O^{2-} ion. One is type-α centre where the O^{2-} ion substitutes for the F^- ion shared by an octahedron of Zn_I site. The other is type-β centre where the O^{2-} ion substitutes for the F^- ion shared by two octahedra of Zn_{II} sites.

The ratios of axial to isotropic hyperfine parameters A_p/A_s are almost the same for centres A, B and C. From this fact the association of a O^{2-} ion by the V^{4+} ion in centre A is confirmed.

Zarkin *et al* reported detailed values of bond lengths and bond angles for the isomorphous fluoride $CsMnF_3$ [15]. As the ratios of the lattice parameter c to a for hexagonal $RbZnF_3$ ($c/a = 2.45$) and $CsMnF_3$ ($c/a = 2.43$) are almost the same [2], we assume that the bond angles in $RbZnF_3$ have similar values to the corresponding bond angles in $CsMnF_3$. Due to Mn^{2+}–Mn^{2+} electrostatic repulsion at sites II, the face-sharing fluorine triangle of Mn_2F_9 unit is smaller than the fluorine triangle sharing the vertices with the octahedra of site I. The declined angle of the Mn_{II}–F bond from the c axis is 59° for a F^- ion in the large triangle and is 46° for a F^- ion in the small triangle in $CsMnF_3$. Similarly, in $VLiOF_8$ complexes in hexagonal $RbZnF_3$ the declined angle of the V–O bond from the c axis in the large triangle is considered to be larger than that in the small triangle. So, we may ascribe centre B with larger tilt angle of the z axis (57.8°) to the type-α $VLiOF_8$ complex and centre C with smaller one (52.7°) to the type-β $VLiOF_8$ complex shown in figure 9. The identified

Table 3. Identifications for the vanadium centres formed in $RbZnF_3$.

Centre	Identification	Symmetry
V-doped		
V^{2+} centre	VF_6 in perovskite type $RbZnF_3$	Cubic
Centre A	VOF_5 in perovskite type $RbZnF_3$	Tetragonal
V, Li-codoped		
Centre B	Type-α $VLiOF_8$ in hexagonal $RbZnF_3$	Monoclinic
Centre C	Type-β $VLiOF_8$ in hexagonal $RbZnF_3$	Monoclinic

structures for the observed vanadium centres are summarized in table 3.

5. Conclusion

In the EPR measurements at room temperature for the $RbZnF_3$ crystal doped only with vanadium, two kinds of vanadium spectra were observed. We identified one spectrum with $S = \frac{3}{2}$ and $I = \frac{7}{2}$ to be the cubic V^{2+} centre substituting for a Zn^{2+} ion and the other spectrum with $S = \frac{1}{2}$ and $I = \frac{7}{2}$ to be the tetragonal V^{4+}–O^{2-} centre substituting for a Zn^{2+}–F^- pair of cubic perovskite type $RbZnF_3$. It is confirmed from the formations of these centres that the cubic perovskite type structure is stable at room temperature similarly to pure crystal when $RbZnF_3$ crystal is doped only with vanadium. On the other hand, two kinds of vanadium spectra with monoclinic symmetry were observed for the crystal codoped with vanadium and lithium. These spectra are ascribed to the V^{4+}–Li^+–O^{2-} complexes formed in the Zn_2F_9 units of the hexagonal $RbZnF_3$ crystal. It is confirmed unambiguously by the preferential formation of the V^{4+}–Li^+ pairs substituting for host Zn^{2+}–Zn^{2+} pairs that the high temperature hexagonal phase of $RbZnF_3$ can be stable even at room temperatures when the crystal is codoped with vanadium and lithium. Models of two monoclinic centres were proposed by the considerations of local structure of Zn_2F_9 unit in the hexagonal $BaTiO_3$ type crystal. The isotropic hyperfine parameters A_s for three types of the V^{4+}–O^{2-} centre are almost the same and their magnitudes are considerably larger than that of the V^{2+} centre in $RbZnF_3$ crystal.

References

[1] Babel D 1967 *Struct. Bonding* **3** 1–87
[2] Babel D 1969 *Z. Anorg. Chem.* **369** 117–30
[3] Daniel Ph, Toulouse J, Gesland J Y and Rousseau M 1995 *Phys. Rev.* B **52** 9129–32
[4] Arakawa M, Ebisu E, Takeuchi H and Mori M 1998 *Modern Applications of EPR/ESR: Proc. 1st Asia Pacific EPR/ESR Symp.* (Singapore: Springer) pp 445–52
[5] Arakawa M, Ebisu H and Takeuchi H 1997 *J. Phys.: Condens. Matter* **9** 5193–204
[6] Davies J J, Smith S R P, Owen J and Hann B F 1972 *J. Phys. C: Solid State Phys.* **5** 245–56
[7] Buzaré J Y, Leble A and Fayet J C 1975 *Phys. Status Solidi* b **67** 445–60
[8] Dance J M and Kerkouri N 1979 *C. R. Acad. Sci. Paris* **289** C425–8
[9] Buzaré J Y and Fayet J C 1974 *C. R. Acad. Sci. Paris* **279** B451–4
[10] Watson R E and Freeman A J 1967 *Hyperfine Interactions* ed A J Freeman and R B Frankel (New York: Academic) pp 53–94
[11] Narayana M and Kevan L 1983 *J. Phys. C: Solid State Phys.* **16** L863–6
[12] Jain V K, Seth V P and Malhotra R K 1984 *J. Phys. Chem. Solids* **45** 529–45
[13] Agarwal O P and Chand P 1984 *Solid State Commun.* **52** 417–21
[14] Alonso P J, Zorita E and Alcalá R 1985 *J. Phys. Chem. Solids* **46** 1351–5
[15] Zarkin A, Lee K and Templeton D H 1962 *J. Chem. Phys.* **37** 697–9